Optimization of the mechanical and antibacterial properties of a Ti-3wt.%Cu alloy through cold rolling and annealing

Hailin Yang[1]*, Mengzhen Zhu[1], Jianying Wang[1], Chenxu Ma[1], Xiongwen Zhou[2], Haixia Xing[3], Erlin Zhang[4]*, Shouxun Ji[5]

1. State Key Laboratory of Powder Metallurgy, Central South University, Changsha 410083, China

2. Department of Prosthodontics, Centre of Stomatology, Xiangya Hospital, Central South University, Changsha, 410008, China

3. School of Materials Science and Engineering, Key Lab for Anisotropy and Texture of Materials, Education Ministry of China, Northeastern University, Shenyang, 110819, China

4. Department of General Dentistry, Peking University School and Hospital of Stomatology, Beijing, 100081, China

5. Brunel Centre for Advanced Solidification Technology (BCAST), Brunel University London, Uxbridge, Middlesex, UB8 3PH, United Kingdom

* Corresponding author: Hailin Yang, E-mail address: y-hailin@csu.edu.cn; Erlin Zhang, E-mail address: zhangel@atm.neu.edu.cn

Abstract:

In this work, a cold rolling with 70% thickness reduction and different annealing temperatures were selected to regulate the microstructure of Ti-3wt.%Cu alloy. Microstructural evolution, mechanical properties and antibacterial properties of the Ti-3wt.% Cu alloy under different conditions were systematically investigated in terms of X-ray diffraction (XRD), scanning electron microscope (SEM), transmission electron microscope (TEM), tensile and antibacterial test. The results indicated that cold rolling could dramatically increase the UTS from 520 MPa to 928 MPa, but reduce the fracture strain from 15.3% to 3.8%. With increasing the annealing temperature from 400 to 800 ℃ for 1 h treatment, the UTS decreased from 744 MPa to 506 MPa and the fracture strain increased from 12.7% to 24.4%. Moreover, the antibacterial properties of the Ti-3wt.%Cu alloy under different conditions showed excellent antibacterial rate (>96.69%). The results also indicated that the excellent combination of strength and ductility of the Ti-3wt.%Cu alloy with cold rolling and following annealing could be achieved in a trade-off by tuning the size and distribution of Ti_2Cu phase, which could increase the applicability of the alloy in clinical practice. More importantly, the antibacterial properties maintained a good stability for the Ti-3wt.%Cu alloy under different conditions. The excellent combination of mechanical properties and antibacterial properties could make the Ti-3wt.%Cu alloy a good candidate for long-term orthopaedic implant application.

Keywords: Titanium alloys; Mechanical properties; Antibacterial property; Microstructure; Plastic deformation; orthopaedic implant application

1. Introduction

Titanium alloys have been widely utilized as dental and orthopaedic implants due to their suitable specific strength, corrosion resistance, and good biocompatibility. It is documented that millions of joint replacement are needed in surgery each year and global metallic implant supply are expected to reach $53 billion by 2024 [1]. However, one of the main reasons resulting in the failure of dental/orthopaedic implantation surgery is postoperative infection caused by indwelling devices [2,3], which is difficult to be solved due to complicated surgical procedures and a following long-term period of antibiotic therapy. As such, the antibacterial and anti-inflammatory is always necessary to avoid bacterial infections during the surgical procedure.

Generally, copper (Cu) is regarded as a toxic element in many cases, but in human body it is a necessary trace element [4]. It is reported that Cu can potentially promote both proliferation and osteogenic differentiation of mesenchymal stem cells [5]. The daily adequate intake of Cu for each adult is at a level of 2–3 mg and the tolerable limit is about 8 mg/day [6]. Moreover, it is generally believed that Cu and Cu^{2+} have a broad antibacterial spectrum and are strong in antimicrobial capability [7,8]. In fact, several antibacterial metallic alloys have been developed through the introduction of Cu into stainless steels and other metallic alloys, in which the precipitation of copper-bearing phase makes the alloys have antibacterial activity [9,10]. Currently, there are increasing interests in developing Ti based alloys with Cu addition to reduce the risk of infection, while the other desired properties offered by Ti alloy are still maintained.

The amount and distribution of Cu bearing phase in Ti-Cu alloys are critical in the enhancement of mechanical property and antibacterial ability. Generally, high volume fraction of Ti_2Cu phase can provide high strength and strong antibacterial ability [11,12], but the ductility is a concern [13,14], and the possibility of cytotoxic effect of the alloy is also another concern [13-15]. It has confirmed that Ti-10wt.%Cu alloy is excellent in *vitro/vivo* antibacterial properties [16], and high strength of 700-800 MPa but only 1% of elongation can be achieved in the alloy, which is the obstacle of the application for

Ti-10wt.%Cu alloy [14]. However, the lower volume fraction of Ti_2Cu phase in Ti-Cu alloys with less Cu always results in the reduction of antibacterial ability. Zhang et al. [17] reported that the Ti-3wt.%Cu alloy only has 35% of antibacterial rate with solution treatment at 900℃/3h, which make Cu-bearing phase dissolve in Ti matrix. However, the subsequent ageing at 400℃/12h enhances the precipitation of Cu-bearing phase, and the increased Cu-bearing phase improves the antibacterial rate more than 99%. A number of investigations have confirmed the Ti-3wt%Cu alloy is non-toxic and side effects, and has good bactericidal effect, excellent mechanical properties and corrosion resistance [17-21]. However, the further increase of mechanical properties and antibacterial ability of the Ti-3wt%Cu alloy is very interesting in promoting the applicability and increasing the competitiveness.

In this work, the Ti–3wt.%Cu alloy is studied using a processing route to tune the Cu-bearing phase, in which the Ti–3 wt.%Cu alloy is cold-rolled with 70% reduction in thickness and then annealed at different temperatures to improve the ductility while maintaining the amount of Cu-bearing phase. The microstructure, mechanical properties and antibacterial ability of the alloy under different conditions are investigated using SEM, TEM and antibacterial evaluation. The discussion focuses on microstructural evolution, mechanisms of strengthening, and the effect of Cu-bearing phase on the antibacterial property of the alloy.

2. Experimental

2.1. Preparation of Ti-3Cu alloys

This experiment was carried out by remelting grade 4 "CPTi" and 99.9999% pure copper rods in a vacuum melting furnace for five times, achieving partial homogenization by turning over the molten alloys between each of the five melting trials, and then remelting and casting the rods in the same furnace. To avoid the potential segregation of Cu in Ti matrix of casting, hot rolling performed repeatedly for homogenization. The composition is measured by inductively coupled plasma-atomic emission spectrometry (ICP) and the results are given in Table 1.

Before cold rolling, the Ti-3wt.%Cu rods were machined to 10 mm thick strips and annealed at 650 ℃ for 2 hrs to relief the residual stress. Subsequently, the strips were rolled to 3 mm in thickness at room temperature, which corresponds to a 70% reduction in thickness. Then, the Ti-3wt.%Cu alloy strips were individually annealed in an electric resistance furnace at a temperature from 400 °C to 800 °C for 1 h, followed by air cooling. The preparation process of the Ti-3wt.%Cu alloy and the sample manufacturing process are schematically shown in Fig. 1.

Table 1 The composition of experimental Ti-3wt.%Cu alloy measured by ICP-AES.

Element (wt.%)	N	C	H	O	Cu	Others	Ti
Ti-3wt.%Cu	<0.0011	<0.036	<0.0011	<0.12	2.92	<0.08	Bal.

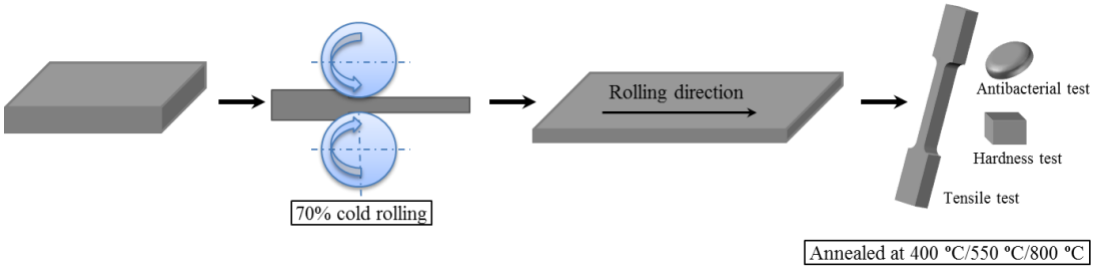

Fig. 1. Schematic diagram showing the preparation process of Ti-3wt.%Cu alloy.

2.2. Microstructure characterization

Phase identification was carried out using x-ray diffraction (XRD, DX-2700BH) ranging from 30 to 80 degree with an accelerating voltage of 40 kV and a current of 30 mA with a scanning step of 0.02°. Specimens for microstructural observation were ground by silicon carbide papers from 400 to 2000 grits and then polished. The microstructural evolution was characterized by scanning electron microscope (SEM, Nova NanoSEM230) with an energy-dispersive x-ray spectrometer (EDS). To further study the deformation mechanisms in the Ti–3wt.%Cu alloy, the detailed microstructure characterization for the specimens after tensile test were examined by transmission electron microscope operating under 200 kV (TEM, Tecnai G2 F20). Prior to TEM observation, the alloys were sliced and ground to 30 μm along the stretching direction from the tensile fracture and thinned in thin foils using the

precision ion polishing system (PIPS) at a voltage of 5 kV and an incident angle of 3 ~ 7°.

2.3. Mechanical properties

Micro-hardness was measured utilizing micro-Vickers hardness tester (HMV-G20, Shimadzu Corporation) with a load of 200 g and a dwell time of 15 s. To ensure the repeatability, the hardness was selected randomly at least 8 different points. The dog-bone-shaped tensile specimens with a gauge length of 30 mm and cross-section of 2.2×1.5 mm^2 were cut using electrical discharge. Then, both sides of the specimens were mechanically ground to a 2000 grit finish with SiC papers. Uniaxial tensile testing was conducted on a Material Testing System (Instron–division of ITW LTD, Model 3369) with engineering strain rates of 1×10^{-3} s^{-1} at room temperature.

2.4. Antibacterial properties

The plate counting method *in vitro* was utilized to evaluate the antibacterial properties of samples. Antibacterial experiments were carried out on the Ti-3wt.%Cu alloy before and after rolling and heat treatment. CP-Ti (Grade 2) was selected as the control group and baseline for comparison. In this study, the antibacterial ability of the alloy was evaluated by the antibacterial effect of the alloy on Gram-positive Staphylococcus aureus (*S. aureus* ATCC25923). The frozen bacterial powder was dissolved in the medium and cultured at 37 ℃ for 24 hrs. After dilution, the bacterial suspension with a concentration of 1×10^5 cfu/ml was obtained [22]. The wafers with a thickness of 2 mm were cut along the direction parallel to the rolling, and three samples were prepared for each group. Before measurement, the individual sample with a size of 15× 2 mm^2, ground with a SiC paper from 400 to 2000 grits. After ultrasonic cleaning with distilled water, the wafers were used for antibacterial performance test. After sterilization and natural drying, the samples were placed in a 24-well plate, 0.1 mL of bacterial suspension droplets were added to the surfaces of all samples and incubated at a constant temperature (37±1℃) for 24 hrs in 5% CO_2 and 90% relative humidity. After the culture was completed, the sample was cleaned

with normal saline for several times, and the washing liquid was stirred homogenously with a vortex oscillator. 0.1 mL of washing solution was taken out and coated on the fixed nutrition washing plate and incubated at 37 ℃ for 24 hrs. The number of active colonies in each sample was counted for six times with an automatic colony counting instrument. The statistical standard was based on GB/T 4789.2-2010 [23] medium and the number of colonies was calculated.

The bactericidal capacity of Ti-3wt.%Cu alloy under different conditions was evaluated based on the number of CP-Ti colonies in the control group under the same culture conditions. The calculation formula is as follows:

$$R(\text{Sterilization rate}) = (N_1 - N_2)/N_1 \times 100\% \quad (1)$$

where N_1 is the number of colonies in the control group; N_2 is the number of colonies in the experimental group.

3. Results

3.1 Microstructure

Fig. 2 shows the XRD spectra of the Ti-3wt.%Cu alloy with different conditions. It can be observed that the diffraction peaks of α-Ti at 38° and 40° were detected. However, there were some of the overlapping diffraction peaks of Ti and Ti_2Cu phases. Due to the low Cu content of 3 wt.%, it was difficult to distinguish the Ti_2Cu phase in the sample before and after cold rolling. It is worth noting that there were no significant shifts of the positions of α-Ti peaks. Furthermore, the diffraction peak corresponding to α-Ti (002) crystal plane was significantly enhanced after cold rolling, suggesting that the preferred orientation appeared after cold rolling. Moreover, the intensity of the diffraction peaks of the (101) crystal plane in the cold rolled alloy was lower than that of the alloy before cold rolling. For the annealed samples, when annealing at 400℃/1 h, the diffraction peaks of α-Ti showed no significant shifts. After annealing at 550℃/1 h, the (002) diffraction peaks of the matrix were obviously weakened, and the (101) diffraction peaks were enhanced, and the peaks of Ti_2Cu were occurred, indicating that the preferred orientation disappeared after cold rolling.

However, when annealing at 800℃/1 h, the diffraction peaks of α-Ti were widened to some extent, and the diffraction peaks of Ti_2Cu were weakened.

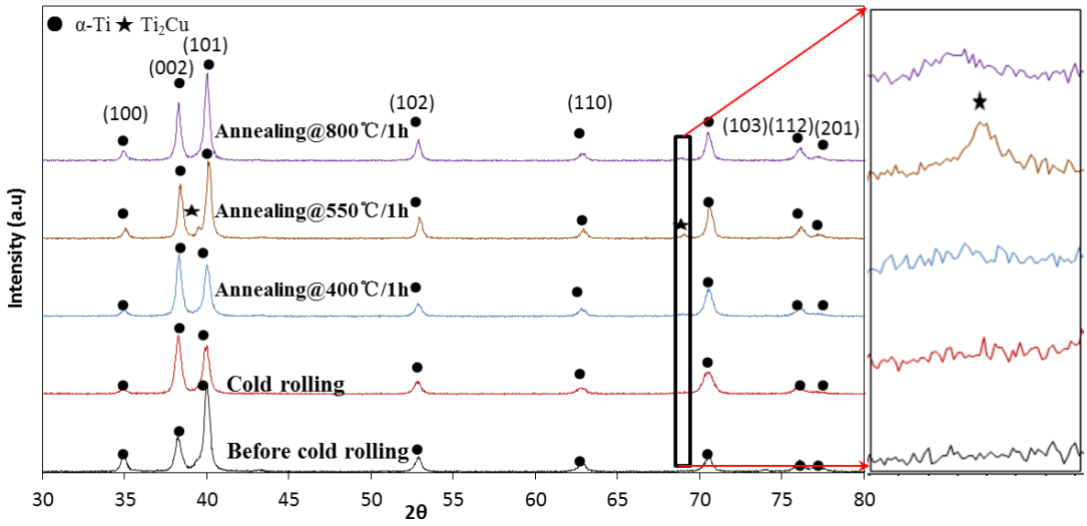

Fig. 2 XRD spectra of the Ti–3wt.%Cu alloy under different conditions.

Fig. 3 shows the microstructure of the Ti–3wt.%Cu alloy under different conditions. In Fig. 3a, the microstructure of Ti–3wt.%Cu alloy before cold rolling typically consisted of light grey α-Ti phase and white band eutectoid Ti_2Cu phase [24]. The discontinuous Ti_2Cu phase band showed an alternative and laminated distribution with α-Ti phase at a width of 2.8 μm. After cold rolling, as shown in Fig.3b, the width of α-Ti phase was reduced to 0.2 μm and the white Ti_2Cu phase band became narrow in comparison with the alloy before cold rolling. Moreover, some of the Ti_2Cu phase showed a continuous distribution along the rolling direction, as indicated in Fig.3b. For the microstructure of the alloy annealed at 400-800 ℃ for 1 h, the preferred orientation was weakened, as shown in Fig.3c and 3d. When annealing at 800 ℃/1 h, as indicated in Fig.3e, the preferred orientation was eliminated. On the other hand, as shown in Fig.3c, the white Ti_2Cu phase bands became coarsened and discontinuous after annealing. As the annealing temperature increased to 550 ℃, part of the Ti_2Cu phase was spheroidized and the white Ti_2Cu phase bands were much coarser and the precipitated Ti_2Cu phase was observed in the α-Ti phase, as indicated in Fig. 3d. When annealing at 800 ℃ / 1h (Fig.3e), the white Ti_2Cu phase became individual globular in shape and discontinuously distributed along the rolling direction.

Moreover, it is noted that the number density of Ti_2Cu phase was much reduced as well (Fig. 3e).

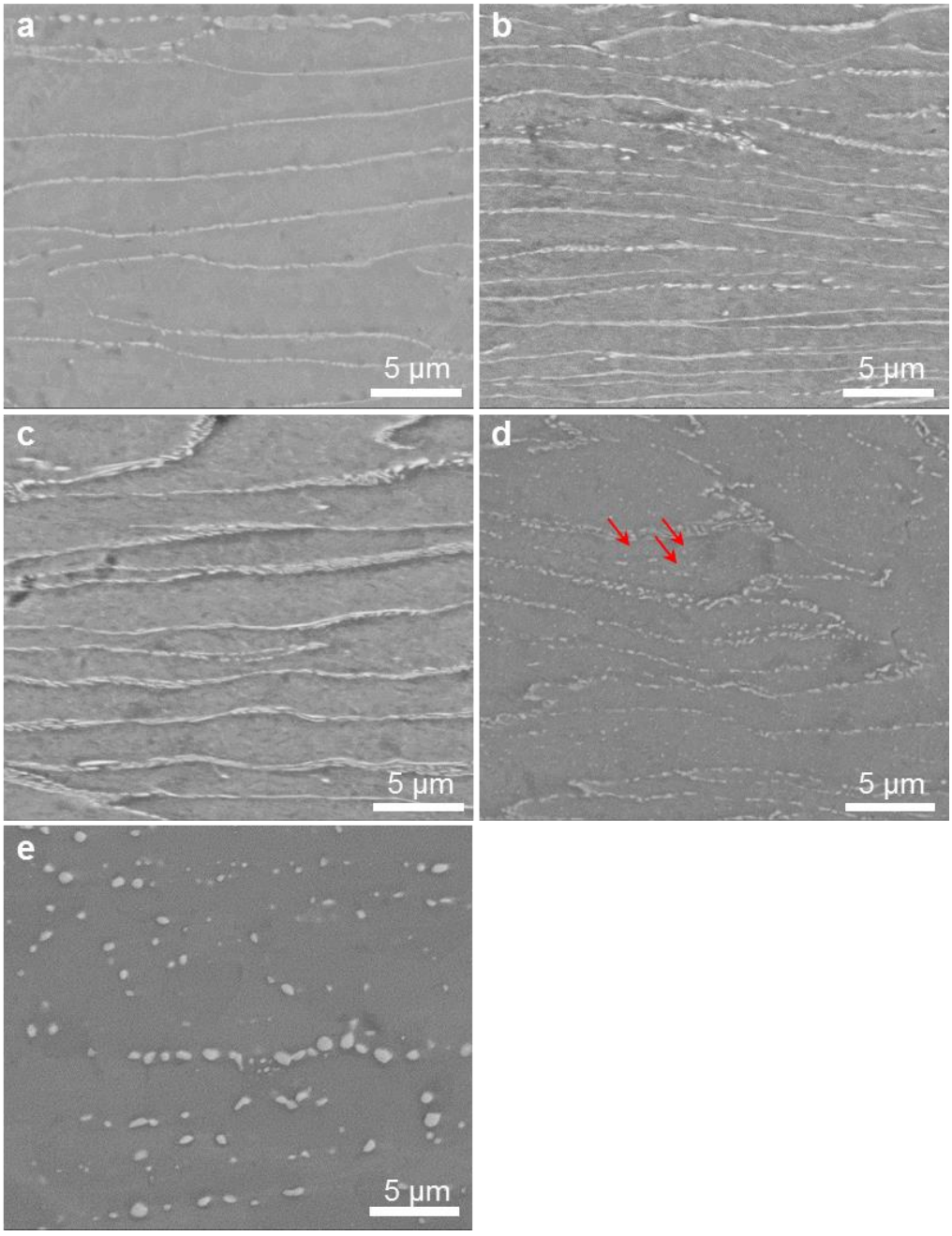

Fig. 3. SEM micrographs showing the microstructure of the Ti–3wt.%Cu alloy under different conditions; (a) Before cold rolling, (b) Cold rolling, (c) Annealing at 400℃ /1h, (d) Annealing at 550℃/1h, (e) Annealing at 800℃/1h.

3.2 Mechanical properties

The variation of Vickers hardness of Ti-3wt.%Cu alloy under different conditions is

shown in Fig. 4 The results revealed that, as expected, cold rolling significantly improved the hardness of the alloy. With cold rolling, the microhardness increased dramatically from 198.1 HV to 308.9 HV. However, when the annealing temperature increased from 400 ℃ to 800 ℃, the microhardness was slightly decreased.

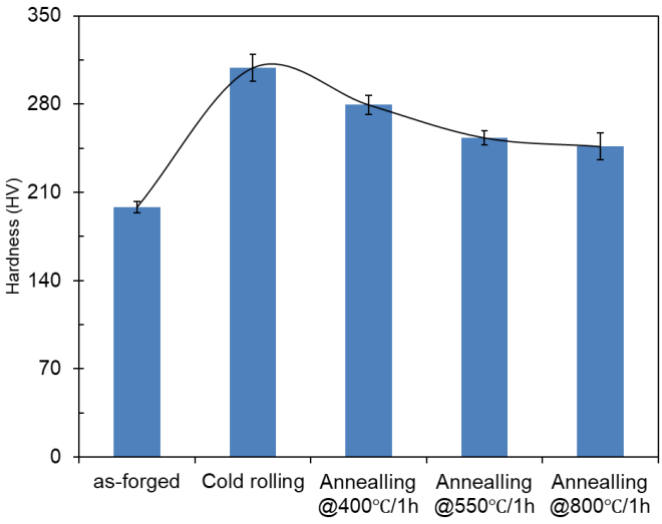

Fig. 4 Hardness of the Ti-3wt.%Cu alloy under different conditions.

The uniaxial stress–strain curves of the Ti-3wt.%Cu ally measured under different conditions are shown in Fig. 5. The yield strength (YS), ultimate tensile stress (UTS) and fracture strain of the alloy before cold rolling were 401.4±2.9 MPa, 520.4±1.4 MPa and 15.3±1.2%, respectively. As cold rolling was applied, the YS of 618.4±15.0 MPa and UTS of 928.7±26.6 MPa were achieved, but the fracture strain was 3.8±0.5 %. When the annealing temperature increased from 400℃ to 800℃, the YS decreased from 612.1±18.0 MPa to 443.6±10.5 MPa, and the UTS decreased from 744.1±1.5 MPa to 506.6±4.0, while the fracture strain increased from 12.7±0.4% to 24.4±3.2%. The detailed mechanical properties of YS, UTS and fracture strain are listed in Table 2 for different conditions. The features of high strength but low ductility were observed in cold rolling sample, but the ductility could be improved by applying annealing at a proper temperature, by which the YS was improved but the fracture strain still remained at a level of that achieved before cold rolling.

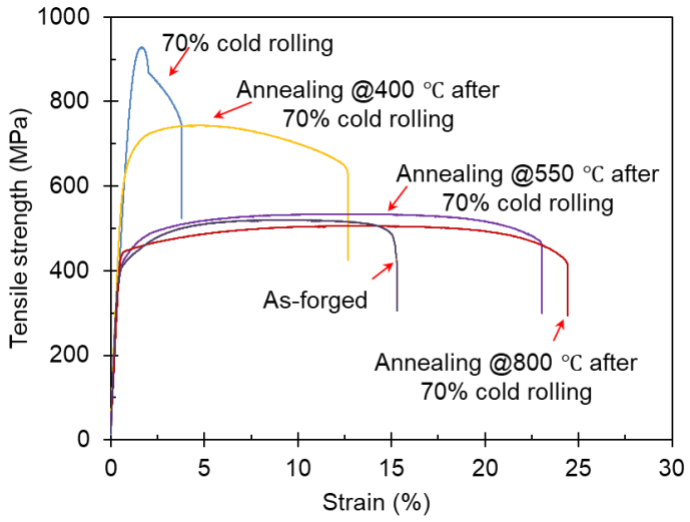

Fig. 5 Tensile stress-strain curves of the Ti-3wt.% Cu alloy under different conditions.

Table. 2 Mechanical properties of YS, UTS, fracture strain of the Ti-3wt.%Cu alloy under different conditions.

	YS (MPa)	UTS (MPa)	Fracture strain(%)	Elastic Modulus (GPa)
Before cold rolling	401.4±2.9	520.4±1.4	15.3±1.2	117.4±1.9
Cold rolling	618.4±15.0	928.7±26.6	3.8±0.5	114.8±0.7
Annealing at 400℃/1h	612.1±18.0	744.1±1.5	12.7±0.4	112.5±0.6
Annealing at 550℃/1h	449.8±16.8	534.4±0.5	23.1±1.1	113.2±5.2
Annealing at 800℃/1h	413.6±10.5	506.6±4.0	24.4±3.2	111.9±10.0

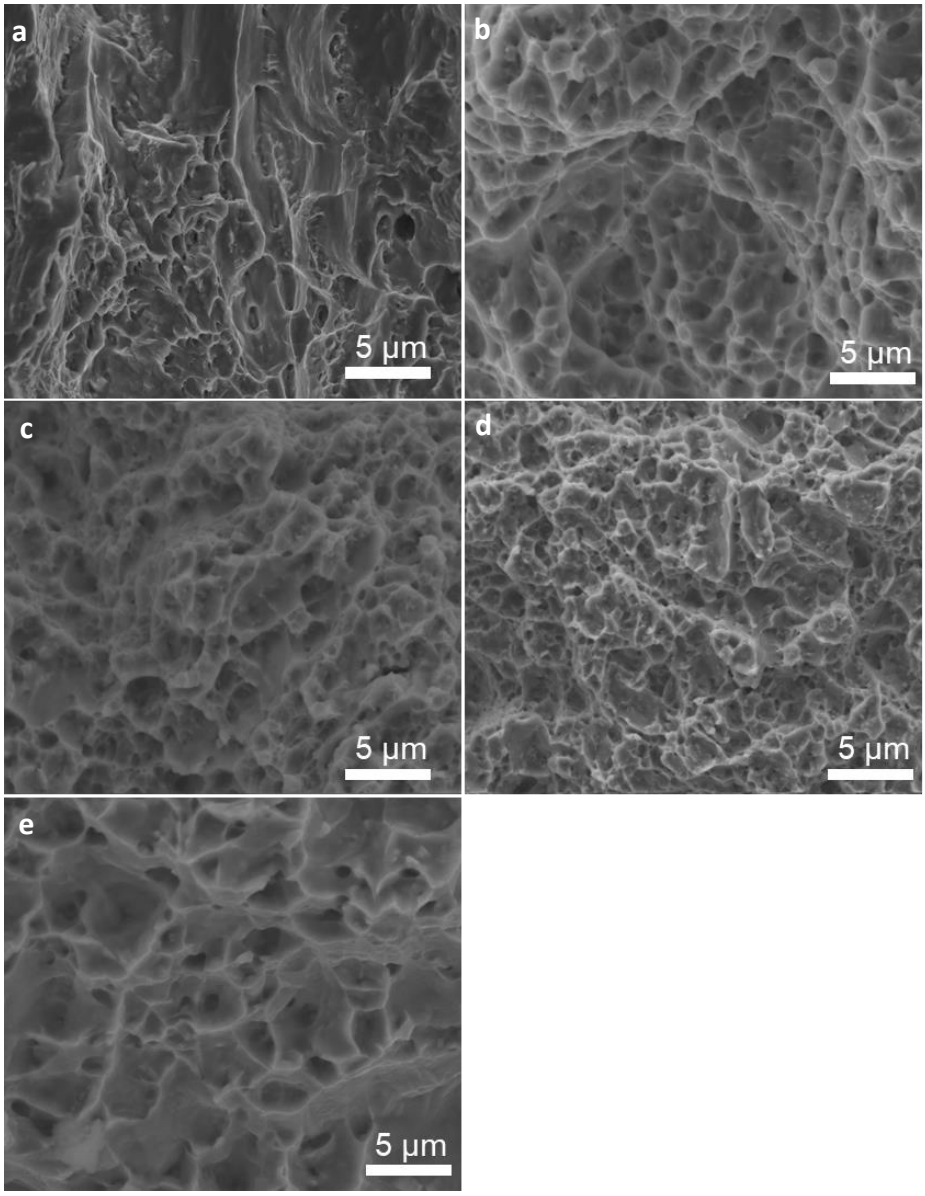

Fig. 6 SEM images showing the fracture morphologies of the Ti-3wt.%Cu alloy under different conditions. (a) Before cold rolling, (b) 70% cold rolling, (c) Annealing at 400°C / 1h, (d) Annealing at 550°C/ 1h, and (e) Annealing at 800°C/ 1h.

Fig. 6 shows the fractographies of the Ti-3wt.%Cu alloy processed under different conditions. It is seen the mixture of long cleave fracture and dimples in the alloy before cold rolling, but the fracture of the samples after cold rolling showed dimples only fracture.

3.3 Antibacterial property

In this work, the general method of *in vitro* plate antibacterial experiment was utilized

to count the bacterial colonies, and the antibacterial rate (R) of all samples was calculated. Fig. 7 shows the antibacterial rate and colony distribution of each sample and commercial pure titanium against *Staphylococcus aureus*. Fig. 8 shows the antibacterial rate against *S. aureus* for the Ti–3wt.%Cu alloy under different conditions. For the CP-Ti in the control group (Fig. 7f), bacterial colonies were widely distributed throughout the medium, indicating that CP-Ti has no function of killing bacteria. In contrast, for the Ti-3wt.%Cu alloys under different conditions, only a few bacterial colonies were observed on the culture medium of these samples (Fig. 7a-e), indicating that these samples exhibited strong antibacterial ability. Moreover, for the Ti-3wt.%Cu alloy samples under different conditions, the difference in the number of bacterial colonies was not significant. However, in the sample annealed at 800℃/1h, the antimicrobial activity slightly decreased (Figs. 7 and 8). This is likely that the annealing temperature was higher than the eutectoid temperature (790℃), which resulted in the re-solutionision of Cu bearing phase into the Ti matrix. According to China's national standard GB4789.2 [25], if R≥90%, the sample has antibacterial ability, and if R≥99%, the sample has strong antibacterial properties. For the Ti-3wt.%Cu alloy under experimental conditions, the antibacterial rate of the samples after annealing at 550 ℃/1h has reached more than 99%, indicating that the samples had strong antibacterial properties, and the antibacterial properties were higher than that of the samples before cold rolling. As shown in Fig. 8, the antimicrobial rates of the other samples also achieved more than 95%, indicating that most of the *S. aureus* cannot survive and reproduce normally on the surface of samples. According to the experimental results, the Ti-3wt.%Cu alloy after cold rolling and annealing still can maintain the excellent antibacterial activity.

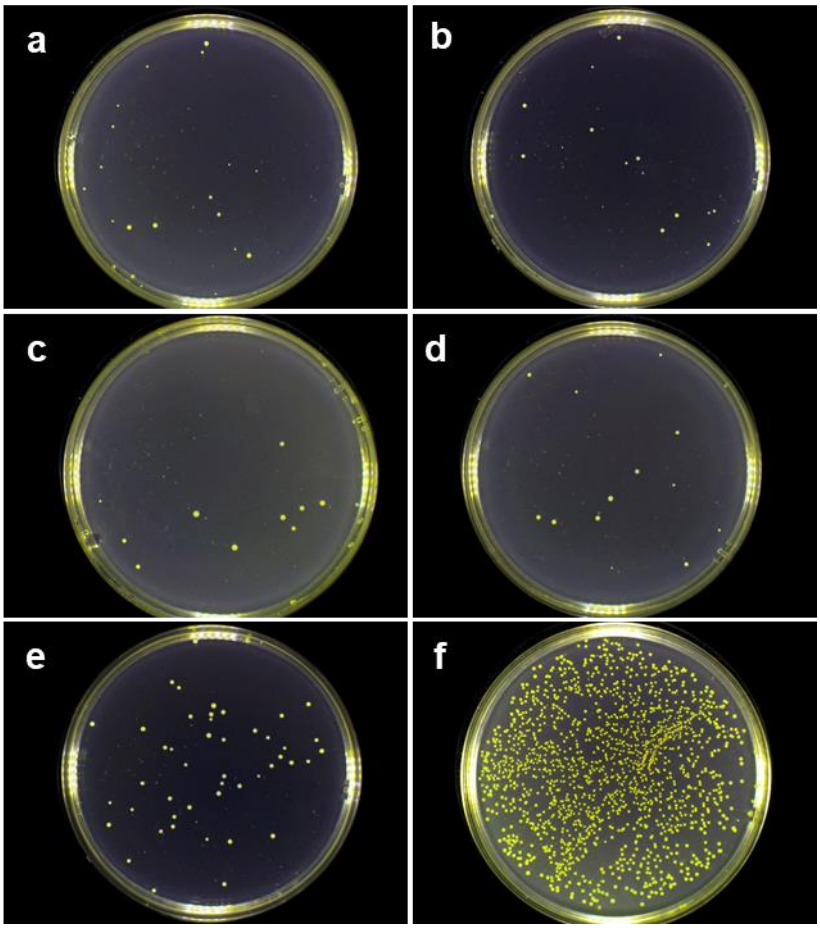

Fig. 7 Antibacterial evaluation results of Ti-3wt.%Cu alloy under different conditions in comparison with CP-Ti. (a) Before cold rolling, (b) Cold rolling (c) Annealing at 400 ℃/1h, (d) Annealing at 550 ℃/1h (e) Annealing at 800 ℃/1h, (f) CP-Ti

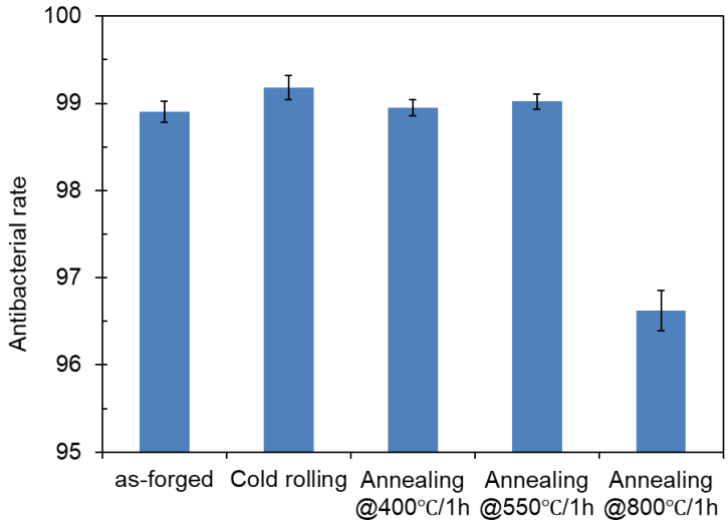

Fig. 8 Antibacterial rate against S. aureus for the Ti–3wt.%Cu alloy under different conditions.

4. Discussion

A combination of strength and ductility can be crucial for a metallic biomaterial. In this work, the effect of cold rolling and following different annealing treatments on the mechanical and antibacterial properties of Ti-3wt.%Cu alloys has been investigated. Clearly, the cold rolling can enhance the strength and the following annealing can effectively achieve a trade-off between the strength and fracture strain while holding the effectiveness of antibacterial ability.

4.1 Mechanism of strengthening/toughening

The Ti-3wt.% Cu alloy is a typical hypoeutectoid alloy and the microstructure is composed of α-Ti and Ti_2Cu phases in the annealed state [26]. The typical band eutectoid microstructure can significantly improve the mechanical properties [27]. Particularly, the Ti-3wt.%Cu alloy annealed at 400 ºC/1h shows YS of 612.1 MPa, UTS of 744.1 MPa and fracture strain of 12.7%.

TEM bright-field images for the Ti–3wt.%Cu alloy before cold rolling after tensile testing are shown in Fig. 9. Similar to the SEM result of Fig. 3a, a typical band eutectoid Ti_2Cu phase can be observed in Fig. 9a. The Ti_2Cu precipitates were also observed by high-resolution TEM and SAED patterns, as shown in Fig. 9b and 9c. It is also seen that the primary β-Ti phase has transformed during eutectoid transformation of β-Ti→α-Ti+Ti_2Cu. Additionally, the band eutectoid Ti_2Cu phase acts as hard phase, interacting with dislocations through the pinning effect and further blocking the dislocations movement, as indicated in Fig. 9d. Therefore, the further cold plastic deformation of Ti-3wt.%Cu alloy was dominantly accommodated by dislocation motion and interaction between dislocations eutectoid Ti_2Cu phases.

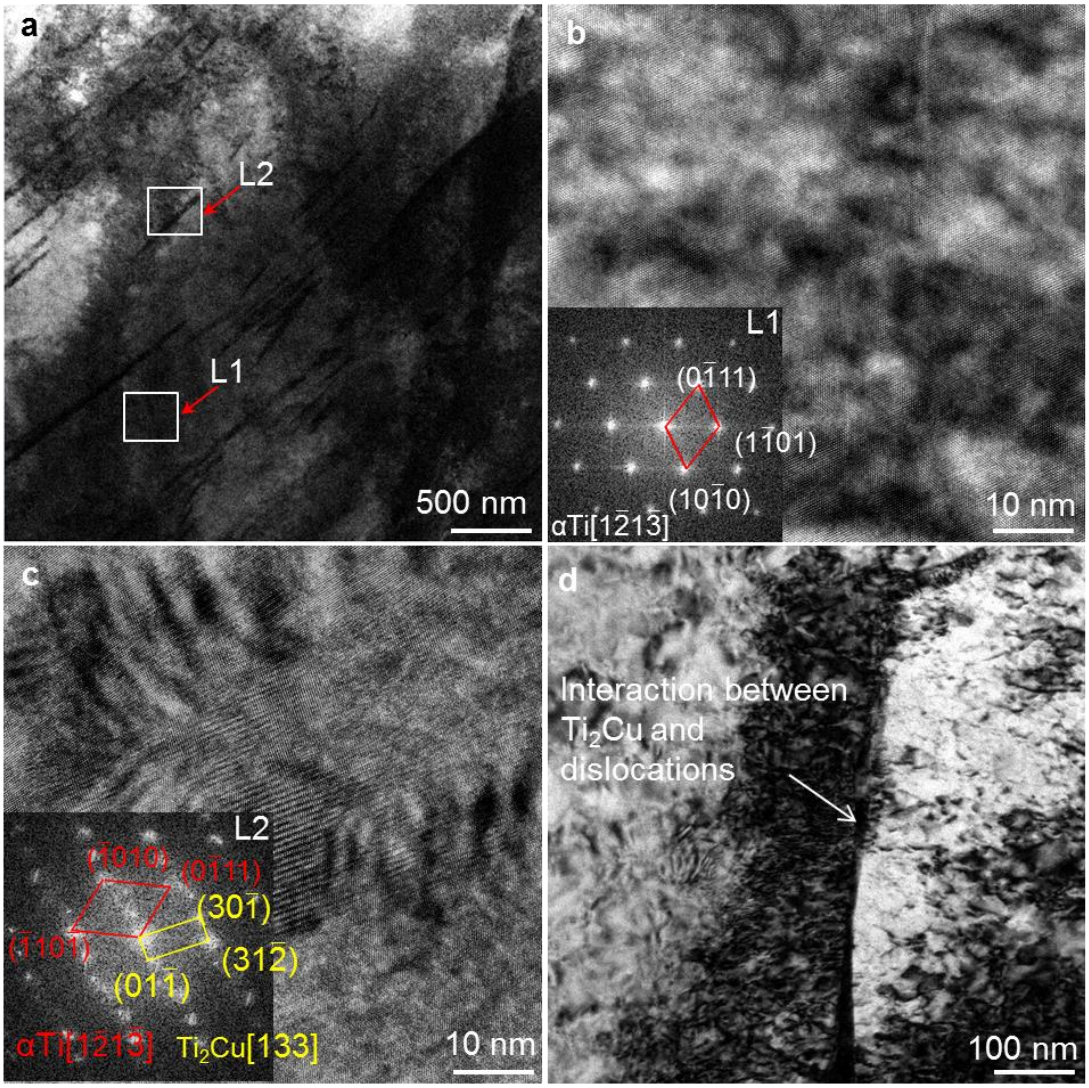

Fig. 9. TEM bright-field images of Ti–3wt.%Cu alloy before cold rolling. (a) TEM Bright-field image of typical band eutectoid Ti_2Cu phase; (b) The high-resolution TEM image with SAED pattern L1, showing α-Ti phase; and (c) The high-resolution TEM image with SAED pattern L2, showing α-Ti phase and Ti_2Cu phases; (d) The interaction between Ti_2Cu phases and dislocations.

In Fig. 5, cold rolling can increase the strength, but decrease the fracture strain of Ti-3wt.%Cu alloy. To understand the dominant strengthening mechanism, microstructure was further analysed in detail. Fig. 10a shows the smaller distance between band eutectoid Ti_2Cu phases in comparison with Ti-3wt.% Cu alloy before cold rolling. According to the classical strengthening theory, the resistance against dislocation movement can be calculated as follows:

$$\tau = Gb/l \quad (2)$$

where τ is the stress for the dislocation movement, G is the shear modulus, b is the Burger vector of dislocation and l is the distance between precipitates.

Obviously, the band eutectoid Ti_2Cu phase with finer space induces higher resistance to dislocation movement. Moreover, the high-resolution TEM and SAED patterns indicate a semi-coherent interface between α-Ti matrix and Ti_2Cu precipitates. Previous studies [28] have confirmed that the misfit dislocations and interface disconnections are critical interfacial dislocations in a semi-coherent interface because these can act as sources for nucleation of lattice dislocation. The interaction between high-density dislocations introduced by semi-coherent interface and Ti_2Cu precipitates deliver higher strength and hardness. However, the severe dislocation pile-up was also observed in the areas near to Ti_2Cu, as shown in Fig. 10c. Although strong blockages of dislocations impinge on the Ti_2Cu and cause mechanical strengthening, the severe dislocation pile-up obviously sacrifices ductility. Therefore, the cold rolled Ti-3Cu samples deliver high UTS of 928.3 MPa with a lower fracture strain of 3.8%.

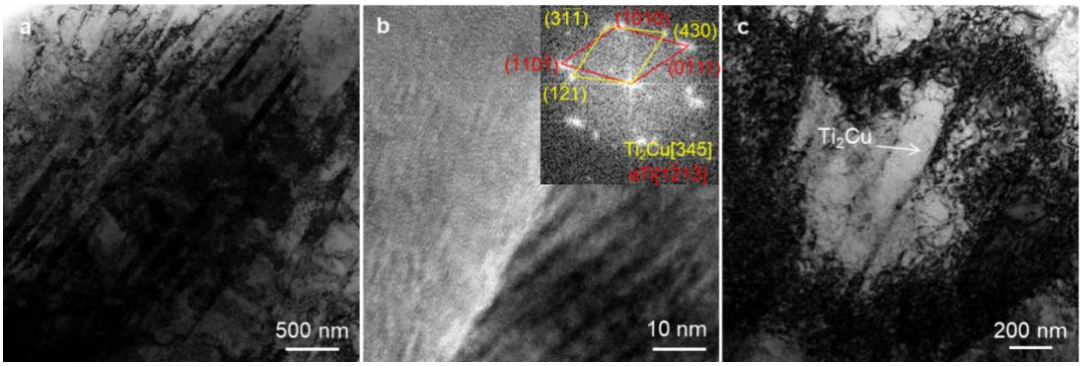

Fig. 10. TEM bright-field images of Ti–3wt.%Cu alloy after cold-rolling. (a) Bright-field image showing the band eutectoid Ti_2Cu phase with finer size; (b) The high-resolution TEM image with SAED pattern, showing α-Ti phase and Ti_2Cu phases; (c) the dislocation cells.

Annealing treatment is an effective approach to tune both strength and ductility. The annealing-induced decrease in strength and increase in ductility are closely associated with the microstructural evolution. TEM analysis of the Ti-3wt.%Cu alloy treated by

cold rolling and annealing at 400 ºC/1 h is shown in Fig. 11. The relatively bigger space between band eutectoid Ti_2Cu phases can be observed in Fig. 11a and 11b in comparison with cold rolling. According to the equation (2), the band eutectoid Ti_2Cu phases with bigger space with annealing at 400 ºC/1 h brought about lower resistance to dislocation movement than those treated by cold rolling. However, a lower density of spherical *in-situ* Ti_2Cu phases interact with dislocations can be detected in Fig. 11c, and corresponding SAED patterns of α-Ti phase and Ti_2Cu phases are shown in Fig. 11d. Although the band eutectoid Ti_2Cu phases with bigger space decreases the Ti-3wt.%Cu alloy, the lower density *in-situ* Ti_2Cu phases can offset the decrease in strength to some extent. Therefore, the samples with annealing at 550 ºC/1 h deliver higher fracture strain of 12.7% with relatively high YS of 612.1 MPa. Additionally, qualitative chemical elemental mapping analysis of the Ti_2Cu phases was also performed using HADDF and the corresponding results are shown in Fig. 11e-g. Obviously, the band phase is apparently enriched in Cu element.

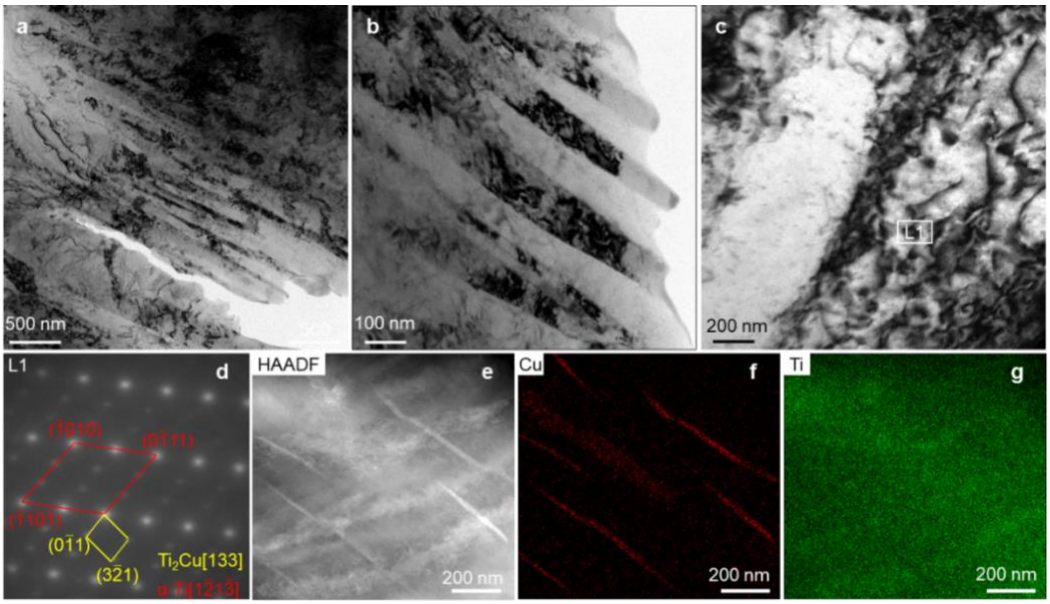

Fig. 11. TEM bright-field images of Ti–3wt.%Cu alloy for the sample annealed at 550 ºC/1 h. (a)-(b) Bright-field image showing the band eutectoid Ti_2Cu phase with relatively large size; (c) the interaction between nano-size Ti_2Cu precipitates; (d) SAED pattern L1 showing α-Ti phase and Ti_2Cu phases; (e) HAADF image and EDS elemental mapping of Ti (f) and Cu (g).

4.2 The effect Ti_2Cu phase on antibacterial property

In this study, it is found that the Ti-3wt.%Cu alloys under different conditions exhibit excellent antibacterial ability (>95%) according to our antibacterial evaluation results, which is an significant improvement comparing with previous reports for the Ti-3wt.%Cu alloy without rolling and annealing [29,30]. The antibacterial mechanism of Cu-bearing phase is not yet fully revealed, however possible mechanisms such as nucleic acids and lipids, oxidation of cell proteins, inhibition of biofilm, damaging DNA, and various essential cell reactions have been proposed [31-36]. According to theses mechanisms, the improved antibacterial ability can be resulted from increasing effective contact, which can inhibit bacteria adhesion on the surface and avoid the formation of bacterial biofilm [37]. It is reported that high Cu content or Ti_2Cu phase can accelerate the release of Cu ion, which implies that the inducing high volume fraction of Ti_2Cu phase from Ti-Cu alloys could offer superior antibacterial [38]. In this work, the samples without and with cold rolling (Fig.3a and 3b) maintain no obvious change of the content of Ti_2Cu phase. Therefore, the antibacterial abilities are expected no obvious change in common sense. However, the cold rolling introduces extra plastic deformation in the alloy and the deformation unavoidably introduces the dislocations in the primary grains. The subsequent annealing can promote the accumulation of dislocations and become low angles grain boundaries. Simuternously, these apply on Ti_2Cu phase, which can be precipitated with finer size with cold plastic deformation. Therefore, the Ti_2Cu phase should be finer in the sample after cold rolling and annealing, which results in the improvement in antibacterial rate, as indicated in Fig. 8. With increasing annealing temperatures, the energy introduced into the sample increased and the growth of precipitates are significant, so the effect of cold rolling introduced effect will disappear, and the antibacterial ability will be reduced or even diminished. These have been observed in the present experimental results as well. When annealing at 800℃/1h, Ti_2Cu phase was coarsened and the content of the Ti_2Cu phase showed an obvious decrease, as shown in Fig.3e. And the improvement is not obvious when the annealing is at high temperatures for the

Ti-3wt.%Cu alloy. As consequence, the combination of rolling and annealing must be accomplished for both mechanical property tuning and the enhancement in antibacterial rate.

5. Conclusions

(a) The introduction of severe plastic deformation through cold rolling and subsequent annealing can improve the ductility and strength of Ti-3wt.%Cu alloy, which is excellent for clinical application. The significant improvement of strength and ductility can be attributed to the accommodation of dislocation motion and the interaction between dislocations in eutectoid Ti_2Cu phases.

(b) By cold rolling and subsequent annealing treatment, Ti_2Cu can be refined to improve the antibacterial property. The antibacterial property decreases with the increase of the size of Ti_2Cu. The excellent combination of mechanical properties and antibacterial properties make the Ti-3wt.%Cu alloy an excellent candidate for long-term orthopaedic implant application.

(c) In the forged Ti-3wt.%Cu alloy, yield strength, UTS and facture strain is 401.4±2.9 MPa, 520.4±1.4 MPa and 15.3±1.2%, respectively. When applying a cold rolling for 70% thickness reduction and annealing at 550 ^{o}C for 1 h, the alloy offers the yield strength of 449.8±16.8 MPa, UTS of 534.4±0.5 MPa and fracture strain of 23.1±1.1%.

(c)

Declaration of Competing Interest

The authors declare that they have no known competing financial interests or personal relationships that could have appeared to influence the work reported in this paper.

Acknowledgments

This work is financially supported by National Natural Science Foundation of China (Grant No. 51404302 and 51801003) and Natural Science Foundation of Hunan

Province (Grant No. 2020JJ4732).

References

[1] Kurtz S, Ong K, Lau E, Mowat F, Halpern M. Projections of Primary and Revision Hip and Knee Arthroplasty in the United States from 2005 to 2030. The Journal of Bone & Joint Surgery. 2007;89(4):780.

[2] Kapadia BH, Berg RA, Daley JA, Fritz J, Bhave A, Mont MA. Periprosthetic joint infection. Lancet. 2016;387:386.

[3] Peel TN, Buising KL, Choong PF. Prosthetic joint infection: challenges of diagnosis and treatment. Anz J Surg. 2011;81(1-2):32.

[4] Hostetler CE, Kincaid RL, Mirando MA. The role of essential trace elements in embryonic and fetal development in livestock. The Veterinary Journal. 2003;166(2):125.

[5] Burghardt I, Lüthen F, Prinz C, Kreikemeyer B, Zietz C, B HN, Rychly J. A dual function of copper in designing regenerative implants. Biomaterials. 2015;44:36.

[6] IPCS(1998).Copper: Environmental Health Criteria 200,Geneva, International Programme on Chemical Safety,World Health Organisation.

[7] Vimbela G, Ngo SM, Fraze C, Yang L, Stout DA. Antibacterial properties and toxicity from metallic nanomaterials. 2017;12:3941.

[8] Zhuang YF, Zhang SY, Yang K, Ren L, Dai KR. Antibacterial activity of copper‐bearing 316L stainless steel for the prevention of implant‐related infection. Journal of Biomedical Materials Research Part B: Applied Biomaterials. 2019;108(2):484.

[9] Ren L, Yang K, Guo L, Chai HW. Preliminary study of anti-infective function of a copper-bearing stainless steel. Materials Science and Engineering: C. 2012;32(5):1204.

[10] Nan L, Liu YQ, Lü MQ, Yang K. Study on antibacterial mechanism of copper-bearing austenitic antibacterial stainless steel by atomic force microscopy. Journal of Materials Science: Materials in Medicine. 2008;19(9):3057.

[11] Ng HP, Nandwana P, Devaraj A, Semblanet M, Nag S, Nakashima PNH, Meher

S, Bettles CJ, Gibson MA, Fraser HL, Muddle BC, Banerjee R. Conjugated precipitation of twin-related α and Ti_2Cu phases in a Ti–25V–3Cu alloy. Acta Mater. 2015;84:457.

[12] Zhuang YF, Ren L, Zhang SY, Wei X, Yang K, Dai KR. Antibacterial effect of a copper-containing titanium alloy against implant-associated infection induced by methicillin-resistant Staphylococcus aureus. Acta Biomater. 2021;119:472.

[13] Bao MM, Liu Y, Wang XY, Yang L, Li SY, Ren J, Qin GW, Zhang EL. Optimization of mechanical properties, biocorrosion properties and antibacterial properties of wrought Ti-3Cu alloy by heat treatment. Bioactive Materials. 2018;3(1):28.

[14] Kikuchi M, Takada Y, Kiyosue S, Yoda M, Woldu M, Cai Z, Okuno O, Okabe T. Mechanical properties and microstructures of cast Ti–Cu alloys. Dent Mater. 2003;19(3):174.

[15] Cremasco A, Messias AD, Esposito AR, Duek EADR, Caram R. Effects of alloying elements on the cytotoxic response of titanium alloys. Materials Science and Engineering: C. 2011;31(5):833.

[16] Wang XY, Dong H, Liu J, Qin GW, Chen DF, Zhang EL. In vivo antibacterial property of Ti-Cu sintered alloy implant. Materials Science and Engineering: C. 2019;100:38.

[17] Zhang EL, Ren J, Li SY, Yang L, Qin GW. Optimization of mechanical properties, biocorrosion properties and antibacterial properties of as-cast Ti-Cu alloys. Biomedical materials (Bristol). 2016;11(6):65001.

[18] Vrancken B, Thijs L, Kruth JP, Van Humbeeck J. Heat treatment of Ti6Al4V produced by Selective Laser Melting: Microstructure and mechanical properties. J Alloy Compd. 2012;541:177.

[19] Fan HY, Yang SF. Effects of direct aging on near-alpha Ti–6Al–2Sn–4Zr–2Mo (Ti-6242) titanium alloy fabricated by selective laser melting (SLM). Materials Science and Engineering: A. 2020;788:139533.

[20] Sercombe T, Jones N, Day R, Kop A. Heat treatment of Ti‐6Al‐7Nb components produced by selective laser melting. Rapid Prototyping J.

2008;14(5):300.

[21] Santos EC, Osakada K, Shiomi M, Kitamura Y, Abe F. Microstructure and mechanical properties of pure titanium models fabricated by selective laser melting. Proceedings of the Institution of Mechanical Engineers Part C Journal of Mechanical Engineering Science. 2004;218(7):711.

[22] Zhang EL, Ren J, Li SY, Yang L, Qin GW. Optimization of mechanical properties, biocorrosion properties and antibacterial properties of as-cast Ti-Cu alloys. Biomed Mater. 2016;11(6):65001.

[23] Ministry of Health of the People's Republic of China National Food Safety Standard Food Microbiological Examination: Aerobic Plate Count GB4789.2-2010.

[24] Zhang EL, Wang XY, Chen M, Hou B. Effect of the existing form of Cu element on the mechanical properties, bio-corrosion and antibacterial properties of Ti-Cu alloys for biomedical application. Materials Science and Engineering: C. 2016;69:1210.

[25] National Standard of the People's Republic of China GB 4789.2-2010.

[26] Bhaskaran TA, Krishnan RV, Ranganathan S. On the decomposition of/3 in some rapidly quenched phase titanium-eutectoid alloys. 1995;26A:1367.

[27] Sun QY, Zhu RH, Gu HC. Monotonic and cyclic behavior of Ti – 2.5Cu alloy at room temperature (293 K) and at 77 K. Mater Lett. 2002;54:164.

[28] Shao S, Wang J, Beyerlein IJ, Misra A. Glide dislocation nucleation from dislocation nodes at semi-coherent {1 1 1} Cu–Ni interfaces. Acta Mater. 2015;98:206.

[29] Zhang ZM, Zheng GT, Li HX, Yang L, Wang XY, Qin GW, Zhang EL. Anti-bacterium influenced corrosion effect of antibacterial Ti-3Cu alloy in Staphylococcus aureus suspension for biomedical application. Materials Science and Engineering: C. 2019;94:376.

[30] Fowler L, Masia N, Cornish LA, Chown LH, Engqvist H, Norgren S, Öhman-Mägi C. Development of Antibacterial Ti-Cux Alloys for Dental Applications: Effects of Ageing for Alloys with Up to 10 wt% Cu. Materials. 2019;12(23):4017.

[31] LI JD, LI YB, WANG XJ, YANG WH, ZHOU G. Antibacterial Effect and the

Mechanism of Cu~(2+), Zn~(2+) Bearing Nano-hydroxyapatite. 2006;01:162.

[32] Maharubin S, Hu YB, Sooriyaarachchi D, Cong WL, Tan GZ. Laser engineered net shaping of antimicrobial and biocompatible titanium-silver alloys. Materials Science and Engineering: C. 2019;105:110059.

[33] Percival SL, Bowler PG, Russell D. Bacterial resistance to silver in wound care. J Hosp Infect. 2005;60(1):1.

[34] Sobczyk-Guzenda A, Szymanski W, Jedrzejczak A, Batory D, Jakubowski W, Owczarek S. Bactericidal and photowetting effects of titanium dioxide coatings doped with iron and copper/fluorine deposited on stainless steel substrates. Surface and Coatings Technology. 2018;347:66.

[35] Wang JW, Zhang SY, Sun ZQ, Wang H, Ren L, Yang K. Optimization of mechanical property, antibacterial property and corrosion resistance of Ti-Cu alloy for dental implant. J Mater Sci Technol. 2019;35(10):2336.

[36] Ren L, Ma Z, Li M, Zhang Y, Liu W, Liao Z, Yang K. Antibacterial Properties of Ti–6Al–4V–xCu Alloys. J Mater Sci Technol. 2014;30(7):699.

[37] Liu R, Tang YL, Zeng LL, Zhao Y, Ma Z, Sun ZQ, Xiang LB, Ren L, Yang K. In vitro and in vivo studies of anti-bacterial copper-bearing titanium alloy for dental application. Dent Mater. 2018;34(8):1112.

[38] Wu JH, Chen KK, Chao CY, Chang YH, Du JK. Effect of Ti_2Cu precipitation on antibacterial property of Ti-5Cu alloy. Materials Science & Engineering C. 2020;108:110433.